THE EDGE PLASMA AND DIVERTOR IN TIBER

W. L. Barr

October 16, 1987

W. L. Barr
Lawrence Livermore National Laboratory
Livermore, CA

Summary

An open divertor configuration has been adopted for TIBER. Most recent designs, including DIII-D [1], NET [2] and CIT [3] use open configurations and rely on a dense edge plasma to shield the plasma from the gas produced at the neutralizer plate. **Fig. 1** shows the DIII-D and TIBER-II configurations on roughly the same scale to allow a comparison of dimensions. Experiments on ASDEX, PDX, D-III, and recently on DIII-D have shown that a dense edge plasma can be produced by re-ionizing most of the gas produced at the plate. This high recycling mode allows a large flux of particles to carry the heat to the plate, so that the mean energy per particle can be low. Erosion of the plate can be greatly reduced if the average impact energy of the ions at the plate can be reduced to near or below the threshold for sputtering of the plate material. The present configuration allows part of the flux of edge plasma ions to be neutralized at the entrance to the pumping duct so that helium is pumped as well as hydrogen. This configuration is shown in **Fig. 2** and has the following features:

* Peak heat loads of about 3 MW/m^2, and less than 4.5 MW/m^2 even if the plasma shifts position by as much as 0.1 m in any direction.

* High gas recycling to reduce sputtering and the erosion of the plates and the production of impurity ions.

* Small vacuum ducts made possible by the high pressure in the ducts that results from the high recycling. Pumping speed is 50 m^3/s and pressure in the vacuum ducts is 40 mTorr.

* At least 0.48m of neutron shielding between plasma and the superconducting magnets.

The Divertor Configuration

The divertor configuration shown in Fig. 2 is intended to help TIBER meet its design goal of ignition in a minimum-size device, and to maintain the required spacing (about 0.5 m) for neutron shielding everywhere between the plasma and the superconducting magnets. The minimum distance that can be allowed between the neutralizer plates and the closed field lines is determined by the need to prevent gas and impurities from reaching the confined plasma. With high recycling at the plates, the plasma temperature and density near the plates will be about 10 eV and 10^{20} m^{-3}, respectively. In such a plasma, the mean free paths (mfp) for ionization of the recycled neutrals are short, with the longest being about 50 mm for the fast neutrals that result from charge exchange (CX). Because the cross section for CX of D^0 and T^0 is larger than that for ionization, multiple CX events can allow deeper penetration than the mfp would suggest. In TIBER's divertor configuration the minimum space between a plate and the confined plasma is 150 mm. This is much greater than any of the relevant mfps when the recycle rate, and therefore the density, is high.

Identical top and bottom divertors are each divided into 16 modules so that each module can be removed between the 16 toroidal field (TF) coils. A slab-shaped vacuum duct under each lower plate connects to a circular vacuum pipe, which leads to an external pumping manifold.

TIBER's first wall is located on magnetic flux surfaces to minimize the particle and heat load to the wall. The separation of the first wall from the confined plasma is several radial decay lengths for both particles and energy. The decay length for
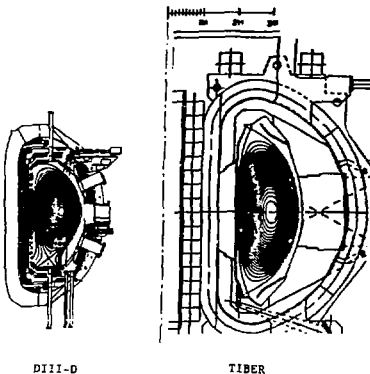

DIII-D   TIBER

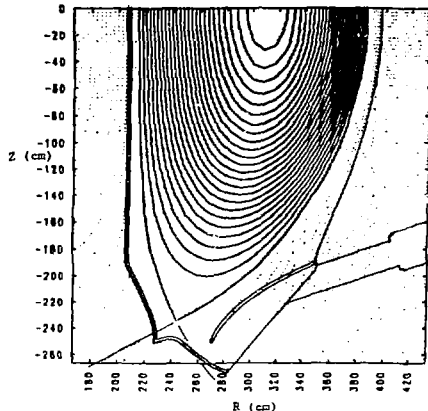Fig. 1. DIII-D and TIBER shown on the same scale for comparison of the divertors.

Fig. 2. The TIBER divertor configuration showing magnetic flux surfaces in the edge plasma and one of 16 vacuum pipes.

energy is about 15 mm at the midplane in both the outer and inner scrape-off layers (SOLs), and the decay lengths for particles are about 20 mm in the outer SOL, and $\Delta_\text{N} \approx 17$ mm in the inner SOL.

The Radial Scale Length for Energy in the Edge Plasma

We calculate the thickness for power flow using a model that includes the variation of thickness caused by variation in the poloidal component of the magnetic field. Fig. 2 shows the large variation in thickness of the magnetic flux tubes in TIBER's SOLs. The primary simplifying assumption made here is that the plasma pressure is constant on a magnetic flux surface. This assumption should be good everywhere except near the divertor plates where a pressure gradient develops to accelerate the new, recycled ions. The constant-p assumption reduces the radial gradients near the null points. We set the total power flow P_SOL into the outer or inner SOL equal to the integral of the cross-field energy transport over the plasma surface facing that SOL:

$$P_\text{SOL} = X_\perp \left[\frac{n_0 k T_0}{\Delta_\text{EO}} \right] 2\pi \int_{n_\text{null.}}^{n_\text{ull+}} \frac{R \cdot B_p}{R_0 \cdot B_{p0}} \cdot R \cdot ds_p ,$$

where s_p is measured along the separatrix in the poloidal plane, and Δ_EO is the radial scale length for energy at the midplane. The integral runs from the lower null point to the upper one. In steady state, half of this power must flow across the sheath at either end of the SOL. Power balance at either sheath requires

$$\gamma c_{s,t} n_t k T_{s,t} A_{+t} = (1/2) P_\text{SOL}$$

Equating these two equations for P_SOL using $A_{+,t} = 2\pi R_0 \Delta_\text{EO} B_{p0}/B_t$, and solving for Δ_EO results in:

$$\Delta_\text{EO} = \sqrt{\frac{X_\perp \cdot L_p}{\gamma \cdot c_s}} \quad \text{where} \quad L_p = \frac{B_t}{B_{p0}} \int_{n_\text{ull.}}^{n_\text{ull+}} \frac{R^2 \cdot B_p}{R_0^2 \cdot B_{p0}} \cdot ds_p .$$

Here, $c_s \approx \sqrt{(2kT_s/M_i)}$ is the ion sound speed; $\gamma = 8$ is the sheath parameter; and subscript t indicates values near the target plate. The uncertainty in this calculation is due mainly to the uncertainty in $X_\perp$, which is expected to range [4,5] from 1 to 4 m^2/s.

Particle and Heat Fluxes to the Walls and Limiters

In normal operation and when the plasma is in its normal position, the particle flux across the inner SOL to the wall armor is determined by the cross-field diffusion rate. We assume Bohm diffusion and write the radial particle flux $\Gamma_\perp$:

$$\Gamma_\perp = - D_\perp \nabla_\perp n \approx \frac{T_e}{16 \cdot B} \frac{n}{\Delta_\text{N}} .$$

Assumed values give $\Gamma_\perp \approx 6 \times 10^{19}$ ions/m^2/s at the wall. Recycling of the resultant gas increases the wall flux by about 40% to $\Gamma_{\perp,w} \approx 1 \times 10^{20}/m^2/s$. Ion impact energy is determined by the local ion temperature and the sheath drop at the wall. This gives an ion impact energy $E_i = 2T_i + 3T_e \approx 400$ eV, while the recycled atoms strike the wall with the energy $E_{at} \approx (3/2)T \approx 120$ eV. The physical sputtering yield for 400 eV D^+ is $Y_{C,D} \approx 0.026$; for 400 eV T^+, it is $Y_{C,T} \approx 0.035$ atoms/ion [6] for normal incidence on carbon. Because the off-normal incident angle could double these yields, we assume a value $Y_C = 0.05$ atoms/ion. For

the 120-eV neutrals the yields are about 0.020 for D^0 and 0.035 for T^0. The resulting erosion rate is 0.8 mm/yr for the graphite armor at the inner wall. Although this erosion rate is serious, it is slow enough to allow convenient scheduling of armor replacement.

At the outer wall the situation is different because the spacing is larger, and because of the poloidal limiters on the outer wall. The spacing between plasma and wall is 120 mm at the outer midplane, and each of the 16 limiters extends inward 20 mm from the wall. A similar calculation as for the inner SOL gives an ion flux of $\Gamma_\perp = 2 \times 10^{19}/m^2/s$ at the radius of the limiters, and a total radial flow of about 2×10^{21} ions/s. The power deposited on the limiters is about 0.13 MW, which gives an average of 8 kW to each of the 16 limiters. The bombarded area on each limiter is determined by the radial distance that the ions diffuse out between limiters. Ion radial velocity due to diffusion is about $v_\perp \approx 59$ m/s, and the time for radial drift between limiters is t ~ $\Delta L/v_\perp \approx 2.3 \times 10^{-5}$ s, which allows a radial drift of $v_\perp t \sim 1.65$ mm. Since the limiters are about 3.8 m long, each limiter has an exposed area normal to the field direction of about $A_{lim} = 6.3 \times 10^{-3}$ m^2. If the heat is divided evenly between the two faces of each limiter, the heat load normal to the field will be 0.6 MW/m^2 on each outer edge of each limiter. This heat does not appear to be a serious problem in normal operation.

Heat Load on the Divertor Plates

The distribution of heat on the divertor plates is calculated by assuming that the energy density in the SOL decreases exponentially with distance out from the plasma at the midplane. This exponential distribution is then mapped, by following magnetic field lines to the divertor plates, to determine the power intercepted by each increment of area on the plates.

Fig. 3a shows the divertor region as modeled by the code. The divertor is specified as a series of coordinate points, and the code calculates the average heat load on each segment and allows adjustment of the shape. Fig. 3b shows the average heat loads plotted against the distance from the separatrix, measured along the surface of the plate. Total power flow in the SOL is set equal to 70% of the total power carried out by charged particles, which is equal to the sum of alpha power, heating power, and current drive power. The other 30% is assumed to be radiated to other surfaces and does not reach the divertors. For Fig. 3, it is further assumed that the SOL power divides with 2/3 of it flowing in the outer SOL and 1/3 flowing in the inner SOL. The results for an 80/20 division of power are obtained by adjusting the vertical scale in the figure. Total charged particle power in TIBER is about 110 MW, with alpha power accounting for about half of it. The three parts of the divertor are labeled "inner," "lower," and "outer."

When the plasma is shifted by 10 cm up or down and/or in or out, the highest heat loads are 4.3 and 4.2 MW/m^2 on the lower plate. These loads occur when the plasma is shifted upward by 10 cm, or radially outward by 10 cm, and when the outer SOL carries 80% of the divertor heat. A worst case would be when this condition exists, and when one null is partially lost so that the heat to the other lower plate increases by 50%. This would give a maximum of 6.6 MW/m^2 on that lower plate.

For normal steady operation we assume that the power divides equally between upper and lower divertors. A perfect 50:50 ratio requires exact symmetry about the midplane. Almost any small asymmetry will result in the path along the field lines to one divertor being shorter than the other.
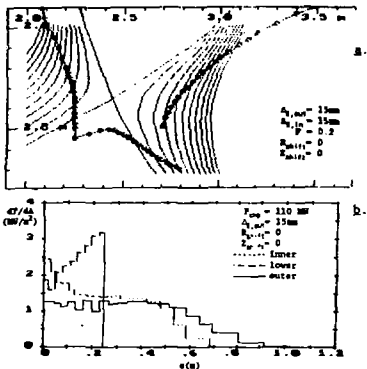
Fig. 3. Heat loads on the divertor plates. **a**. The coordinate points used in the flux mapping of the power flow. **b**. Average heat loads on segments of the plates between coordinate points. Distance s is measured along the surface away from the intersection with the separatrix.

This effect is amplified by the shallow pitch angle due to the weak poloidal field near the nulls. A large deviation from symmetry could destroy one null and allow the other divertor to act as a limiter. Assuming that we can avoid the complete loss of either null, the extreme ratio of power to the two divertors that we might expect is about 25/75.

Particle and Energy Transport in the Edge Plasma

The density and temperature in the SOL are about $n \approx 5 \times 10^{19}/m^3$ and $T_e \approx 100$ eV. In this plasma the mfp for electron-electron scattering is $\lambda_{ee}(m) = 1 \times 10^{16}$ $T_e^2/n_e \approx 2$ m, and $\lambda_{ii} \approx \lambda_{ee}$. Close to the divertor the mfps become shorter. Since these are smaller than the scale length for temperature gradients, we can assume to good approximation that ions and electrons have Maxwellian velocity distributions. However, the mfp for ions to thermalize with electrons varies from about 10 m near the midplane to a few centimeters near the divertors. Therefore, the electron and ion temperatures will be different in the hotter part of the SOL, but will approach equality near the divertor. We assume no net particle flow and only classical electron thermal conductivity in "Region I," the main part of the SOL, but use a fluid model in "Region II" near the divertor.

Power Flow in Region I

Region I ($0 \le s \le s_{dp}$) has an energy source, $q(s)$, but no particle source and no particle flow. The energy equation after a first integration is

$$- A_m(s) K T^{5/2} \frac{dT}{ds} = \int_0^s A_m(s') q(s') ds' .$$

since $[dT/ds]_{s=0} = 0$. This can be integrated again to give

$$T^{7/2}(s) - T^{7/2}(s_{dp}) = -\frac{7}{2K} \int_0^s Q_m(s') ds' ,$$

where we have set

$$Q_m(s) = \frac{1}{A_m(s)} \int_0^s A_m(s') q(s') ds' .$$

This gives the temperature variation along the field line in Region I, and in particular, determines the temperature difference between midplane ($s = 0$) and the beginning of Region II ($s = s_{dp}$). The solutions in Region I and Region II must join smoothly at $s = s_{dp}$.

Power Flow in Region II

The energy equation in Region II has a particle source and particle flow, but no energy source term. After setting $U = T^{7/2}$ and $U' = dU/ds$, the energy equation becomes:

$$U'(s) = (A_{m,dp}/A_m)U'(s_{dp}) + (7/2K) \cdot [5T(s) + E_r] \cdot \Gamma(s).$$

The numerical integration of this equation is iterated until the value of $U(s_{dp})$ agrees with the power input to the SOL and there is power, pressure, and particle balance at the sheath.

Boundary Conditions at the Sheath

The boundary conditions at the sheath at $s = s_L$ are determined by the requirements that particle, pressure, and energy all balance there. Particle balance requires that:

$$\Gamma_{sh} = \frac{1}{A_m(s)} \int_{s_{dp}}^{s_L} A_m(s) S[T(s), n_0(s), p(s)] ds$$

Energy balance at the sheath requires that:

$$\gamma \Gamma(s_L) T(s_L) = -\frac{2K}{7} \frac{dT^{7/2}}{ds} \Big|_{s_L, x} + 5\Gamma(s_L) T(s_L) ,$$

which establishes the relation between heat conduction and convection into the sheath.

Vacuum Pumping at the Divertor

Gas recycling at the lower divertor plate near the duct opening is provided partly by gas from nearby regions of the plate, but mostly by gas from the duct itself. Only a small fraction of the ions entering the duct is removed by the vacuum pumps. The larger fraction enters the plasma and is recycled, so the opening to the duct recycles gas nearly as efficiently as the solid plate. The particle flux at the plate and parallel to the field lines is estimated from the heat flux. $\Gamma_{m,sh} \approx 5 \times 10^{23}$ ions/s/m^2. The width of the magnetic flux tube that carries ions onto the lower plate near the duct is about 130 mm and extends around the machine, giving it an area of $A_{flux} \sim 2.2$ m^2. Since most of the ions that are neutralized here become gas molecules in the duct, the rate of gas input into the duct is

$$\Gamma_{sh} \cdot A_{flux} \sim 1.1 \times 10^{24} \text{ atoms/s} .$$

This gas input rate must be balanced in steady state by the removal rate back into the plasma and out to the pump. The pumping speed of the plasma through the opening A_{plasma} is

$$S_{plasma} = (1/4) \cdot v_{mo} \cdot (1 - R_{plasma}) \cdot A_{plasma} .$$

If we assume that the albedo of the plasma is $R_{plasma} = 0.4$ and take $A_{plasma} = 3.4$ m^2 as shown in Fig. 2,

then $S_{plasma} \approx 640$ m³/s. Notice that $S_{plasma} \gg C_{pump}$ ≈ 25 m³/s for the lower divertor, so S_{plasma} essentially determines the molecular density in the duct. Particle balance requires

$$Q_{out} = 2 \cdot n_{mo} \cdot (S_{plasma} + S_{pump}) = Q_{in} = 1.1 \times 10^{24} \text{atoms/s},$$

which gives $n_{mo} = 8.7 \times 10^{20}$ molecules/m³ for the gas density in the duct and corresponds to a duct pressure of 42 mTorr when the temperature is 500 K. At this high density, the gas conductance should be treated as a viscous flow rather than molecular flow as assumed here. Since the gas conductance of a given geometry is greater in the viscous regime, we designed for the molecular regime to be conservative.

The vacuum pumping system in TIBER must provide the necessary pumping speed for deuterium and tritium and for helium ash in three different stages of operation: (1) initial pumpdown, (2) steady-state plasma operation, and (3) pulsed plasma operation. During initial pumpdown, the gas pressure p in the torus decreases with time t as:

$$p(t) = [p(0) - Q_{og}/S]e^{-t/\tau} + Q_{og}/S .$$

where the pumping speed $S = 50$ m³/s, and the pumping time constant $\tau = V/S = 2.5$ s. The volume $V = 125$ m³, and includes only the inside of the torus since the spaces between shielding modules and behind and around divertor modules are pumped separately by the external system for the superconducting magnets. The gas load on the system during pumpdown, Q_{og}, is due to outgassing of surfaces. Clean stainless steel that has been baked and glow discharge cleaned outgasses at about 10^{-7} Torr-L/s·m² [2, 7]. Moderately clean surfaces before baking can have a rate that is 100 times higher. Again we assume that only the inner surfaces of the torus plus the inner surfaces of the ducts will contribute to the gas load. The inner surface area of the torus is about 200 m² and the total for the ducts and pipes is about 160 m² which totals about 360 m² for outgassing. This gives $Q_{og} \approx 3.6 \times 10^{-5}$ to 3.6×10^{-3} Torr-L/s, and $p(\infty) = Q_{og}/S \approx 10^{-9}$ to 10^{-7} Torr. This base pressure meets the NET goal of 10^{-7} to 10^{-8} Torr after baking and glow discharge cleaning.

The gas load under steady-state plasma operation is just equal to the gas equivalent of the net fueling, plus the gas that is injected into the SOL with the pellets. The net fueling current is about 350 A_s of D⁰ and T⁰, and the extra pellet gas is estimated to add another 420 A_s, or $Q = 68$ Torr-L/s of molecular gas. This gives a pressure in the duct of $P_{duct} = Q/S = 1.4 \times 10^{-3}$ Torr, which is lower than that required for the desired high recycling. This pumping speed is sufficient to allow throttling of the pumps to control the pressure in the duct. In steady state, the He pressure in the duct and the relative concentration of He in the edge plasma near the plates will adjust until He atoms are removed at the rate that α-particles are produced. Our estimate is that the edge plasma will contain about 5% He.

In pulsed plasma operation, the pressure $p(t_d)$ at the end of a dwell time t_d after a pulse is:

$$p(t_d) = [p(0) - p(\infty)]e^{-t/\tau} + p(\infty) \approx p(0)e^{-t/\tau} .$$

with $t = t_d$ and $p(0) = 5 \times 10^{-4}$ Torr is the pressure in the torus at the end of the previous pulse [2]. This equation gives $p(t_d) \approx 2 \times 10^{-6}$ Torr if we assume $t_d = 20$ sec as for NET. This meets the NET goal of 3×10^{-5} Torr, and the 1×10^{-5} Torr design requirement used in the FEDC tokamak systems code [8].

References

1. M. Ali Mahdavi et. al., "Recent Results of Divertor Experiments on DIII-D," GA Technologies Inc., San Diego, CA, Report No. GA-A18909, July 1987.

2. The NET Team, "NET Status Report," c/o Max-Planck-Institute, Garching, West Germany, NET Report 51, Dec. 1985.

3. D.E. Post,"Tokamak Plasma Edge Physics and Impurity Control," Seminar at Lawrence Livermore National Laboratory, Livermore, CA, May 16, 1986.

4. P.J. Harbour, "Thickness of the Scrape-Off Layer of a Large Tokamak," Nucl. Fusion 24, 1211 (1984).

5. P.C. Stangeby, "The Plasma Sheath", in "Physics of Plasma-Wall Interactions in Controlled Fusion", Edited by D. E. Post and R. Behrisch, (Plenum Publishing Corp., 1986).

6. J. Roth, J. Bohdansky, and W. Ottenberger, "Data on Low Energy Light Ion Sputtering," Max-Planck-Institute, Garching, West Germany, Report IPP 9/26, May 1979.

7. T. Batzer, Lawrence Livermore National Laboratory, Livermore, CA, private communication, July 1986.

8. R.L. Reid, et al.,"The Tokamak Systems Code", Fusion Engineering Design Center, Oak Ridge, TN, Report ORNL/FEDC-84/9, pp. 312-326.

DISCLAIMER